Mingling Light, Oxygen, and Organometallics to Form Cobalt-Carbon Bonds in the Confines of a Metal-Organic Nanocage

Daniel A. Rothschild, Aaron Tran, and Mark C. Lipke*

Department of Chemistry and Chemical Biology, Rutgers, The State University of New Jersey, 123 Bevier Road, Piscataway, New Jersey 08854, United States

ABSTRACT: First-row transition-metal complexes often show a propensity for forming reactive radical species, such as superoxide complexes (M–O_2•) generated by the binding of O_2 to the metal, or free alkyl-radicals formed via M–C homolysis. Such radicals are important intermediates in reactions catalyzed by synthetic metal complexes and metalloenzymes, but their high reactivity can lead to undesired side reactions such as quenching by solvent, oxygen, or other radicals. In this work, we show that confinement of a Co^{II} porphyrin complex in a large porphyrin-walled M_8L_6 nanocage allows for the taming of radical reactivity to enable clean oxidative alkylation of the cobalt center with tetraalkyltin reagents via an unexpected process mediated by O_2 and light, which usually promote homolytic decomposition of porphyrin-supported Co^{III}–alkyl bonds. Indeed, analogous Co^{III}–alkyl complexes in free solution degrade too quickly under the alkylating conditions to enable their clean formation. The nanocage also acts as a size-selective barrier for alkylating agents, allowing Co^{III}–alkyl formation using $SnMe_4$ and $SnEt_4$ but not $SnBu_4$. Likewise, Co–C homolysis is facilitated by the persist radical reagent TEMPO but not by a bulky derivative of TEMPO. These results show that nanoconfinement is a promising strategy for guiding radical-based organometallic reactivity under otherwise prohibitive conditions.

Introduction.

Radicals centered on light p-block elements (e.g., C, N, O) are among the most reactive species known in chemistry owing to the typically low kinetic barriers and favorable thermodynamics for engaging the unpaired electron in bonding.[1] Usefully, such radicals can be generated and/or captured by transition metal complexes, especially those involving first-row metals,[2] thereby enabling powerful catalytic methods[3] that include C–H oxidations[4] and C–C cross-coupling reactions.[5] However, the indiscriminate reactivity of radicals limits these methodologies, often leading to low selectivities and restricting suitable reaction conditions or substrates.[6] Thus, it would be desirable to develop new methods for controlling the reactivity of radical intermediates generated by transition metal complexes.

A number of metalloenzymes overcome the challenges of radical-based chemistry by guiding the reactivity of radical intermediates in confined active sites.[7] Many oxygenases precisely control the substrate binding and radical rebound steps of M=O mediated H-atom abstraction processes,[8] and certain B_{12}-dependent enzymes utilize Co–C bond homolysis to release an adenosyl radical that effects 1,2-rearrangements of bound substrates before reassembly of the initial Co–C bond.[9] Molecular nanocages[10] and other nanoporous structures[11] feature cavities that might similarly be used to guide reactivity between radicals and

Scheme 1. Radical reactivity in a porphyrin nanocube.

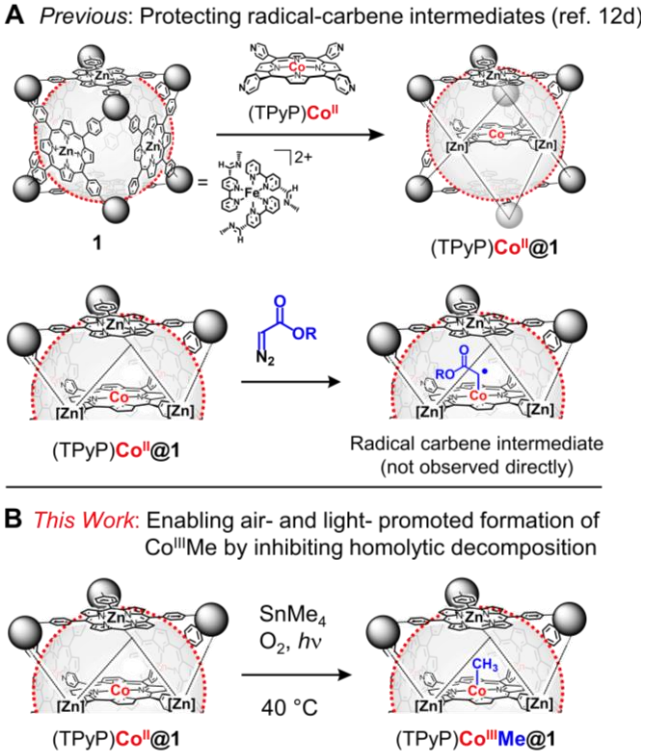

metal complexes, but few examples have been reported[12] even though stabilizing radicals[13] and other reactive species[14] or otherwise guiding reactivity[15] in porous materials is well precedented. In one notable study, de Bruin and Reek increased the TONs of cyclopropanations and intramolecular CH activations by confining a cobalt-porphyrin catalyst in a large nanocube (**1**) comprising six porphyrin walls bound together by eight $(bipy)_3Fe^{2+}$ vertices that are connected to the porphyrins via imine linkages (Scheme 1A).[12d] These connections are dynamic enough to allow uptake of a $[(4\text{-py})_4\text{porphyrin}]Co^{II}$ guest ($TPyPCo^{II}$), providing a way to isolate this catalyst inside the cube to stabilize radical-carbene ligands against detrimental radical dimerizations.[12d,16] This example exclusively involves metal-bound radicals, in contrast to the fully organic radical intermediates generated by H-atom abstraction or M–C homolysis. The ability of artificial porous materials to guide the reactivity of free alkyl radicals may, however, be responsible for the improved selectivity of C–H halogenations in a metal-organic framework reported by Li and Zhou, though we can only speculate since no mechanistic details were examined.[17]

Given the scarcity of studies involving main-group radicals and transition metals in nanoporous structures, we became interested in identifying a system in which metal/radical reactivity could be examined in a confined space, focusing on stoichiometric reactivity to complement the aforementioned catalytic studies. Porphyrin-supported $Co^{III}R$ complexes (R = alkyl) can undergo thermally or photolytically induced Co–C homolysis,[2c] so $Co^{III}R$ derivatives of de Bruin's and Reek's encapsulated cobalt-porphyrin complex were targeted as precursors that are susceptible to generating free alkyl radicals (R•) in a well-defined nanopore. However, the cubic cage is not stable to typical conditions for forming $Co^{III}R$ complexes, necessitating identification of other methods for forming Co^{III}–C bonds. Serendipitously, we discovered a new process for 1 e^- oxidative alkylation of Co^{II} porphyrin complexes with tetraalkyltin reagents using light and O_2 as promoters (Scheme 1B), conditions which usually destabilize Co–alkyl bonds.[18] Indeed, alkylation of unencapsulated cobalt porphyrins was less effective using these conditions due to degradation of the products back to the Co^{II} state. Additionally, the cage acts as a size-selective barrier for alkylating the encapsulated Co^{II} site with SnR_4 and for controlling the reactivity between the Co^{III}–R complexes and persistent radicals such as O_2 and derivatives of TEMPO.

Results and Discussion.

Alkylation of an encapsulated Co porphyrin complex. The cubic cage **1** presents a challenge to alkylation of the encapsulated (TPyP)Co complex via common methods for preparing cobalt alkyl complexes. For example, the redox-active $(bipy)_3Fe^{2+}$ linkers prevent selective reduction of Co^{II} to Co^{I}, ruling out oxidative addition of alkyl halides to Co^{I} as a route to prepare $Co^{III}R$ complexes.[19] Additionally, **1** is only soluble in solvents (e.g., DMF, MeCN) that are incompatible with alkyl anion reagents (e.g., Li–alkyl, XMg–alkyl) that are often used to form $Co^{III}R$ complexes via metathesis with $Co^{III}X$ starting materials.[20] Therefore, we targeted alkylation of encapsulated $(TPyP)Co^{III}Cl$ complexes using alkyltin reagents (SnR_4) that are minimally nucleophilic but which have been reported to participate in metathesis with Co^{III}–Cl to form Co–C bonds and R_3SnCl.[21]

Encapsulation of $(TPyP)Co^{III}Cl$ was attempted using the reported conditions for uptake of $(TPyP)Co^{II}$ into the cubic cage.[12d] A stoichiometric amount of $(TPyP)Co^{III}Cl$ was suspended in a DMF solution of the cube and heated at 70 °C for 36 h under N_2. However, the ^{1}H NMR spectrum of the product (Figures 1A and S1) lacks the upfield shifted pyridyl and pyrrolic CH resonances reported for other diamagnetic porphyrin complexes bound in the cubic cage.[12d] Instead, the spectrum matched that reported for the complex of $(TPyP)Co^{II}$ in the cube, suggesting reduction of the $Co^{III}Cl$ complex during encapsulation. Likewise, only the Co^{II} state of the host-guest complex was observed by ESI-HRMS (Figure S30), and EPR spectroscopy showed a l.s. Co^{II} signal matching that reported for **$(TPyP)Co^{II}$@1** (Figure S34).[12d] Lastly, **$(TPyP)Co^{II}$@1** was intentionally prepared and exhibited ^{1}H NMR characterization data matching that of the product of our attempts at encapsulating $(TPyP)Co^{III}Cl$ (Figures 1A,B). It is unclear exactly how the $(TPyP)Co^{III}Cl$ complex is reduced upon encapsulation, but it is conceivable that the 16+ charge of the cube and the coordination of the pyridyl groups of the TPyP ligand to the Zn centers of the cube raise the $Co^{III/II}$ reduction potential, destabilizing the Co^{III} state.

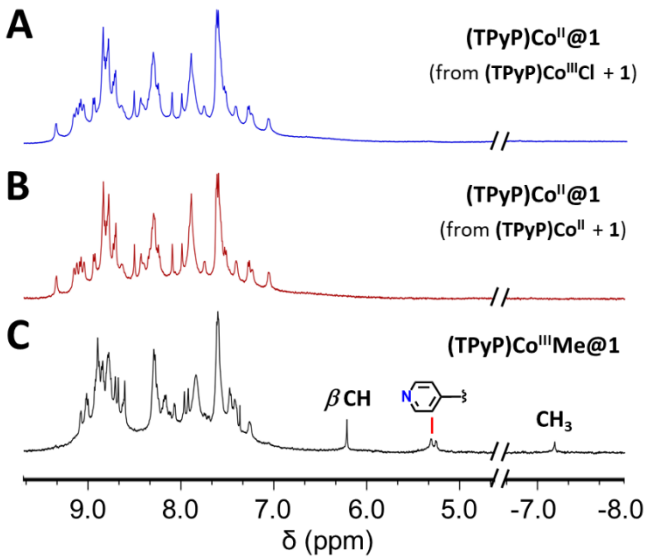

Figure 1. Truncated ^{1}H NMR spectra of (A) **$(TPyP)Co^{II}$@1** formed from $(TPyP)Co^{III}Cl$ and **1**; (B) **$(TPyP)Co^{II}$@1** formed from $(TPyP)Co^{II}$ and **1**; and (C) **$(TPyP)Co^{III}Me$@1** with signals of the TPyP β CH positions, the 3-positions of the pyridyl groups, and the methyl ligand indicated. All spectra were recorded in CD_3CN at 25 °C on a 500 MHz instrument.

Fortuitously, we attempted to methylate the encapsulated cobalt complex with $SnMe_4$ prior to realizing the expected $Co^{III}Cl$ state had been reduced to Co^{II}, which surprisingly still led to formation of the desired Co^{III}–Me complex. The methyl ligand was identified by the appearance of a signal at –7.17 ppm in the ^1H NMR spectrum of the product (Figures 1C, S2, and S3), and signals of the pyridyl and pyrrolic CH positions of the TPyP ligand were respectively seen at 5.28 and 6.21 ppm (Figures 1C, S2, and S3), consistent with binding of a diamagnetic porphyrin complex in the cube. The DOSY separated ^1H NMR spectrum revealed another resonance at 2.33 ppm (Figure 2) that had been hidden by the water residual signal. This resonance corresponds to the 2-position CH bonds of the TPyP pyridyl groups, filling in all the expected resonances of the encapsulated (TPyP)Co^{III}Me complex. ESI-HRMS confirmed the identity of this host-guest complex (Figures 3 and S31), showing that the Co^{III}–Me bond survives even in the gas phase, suggesting it is stabilized in the cube since we were unable to observe related monomeric Co^{III}Me complexes by HRMS under analogous conditions.

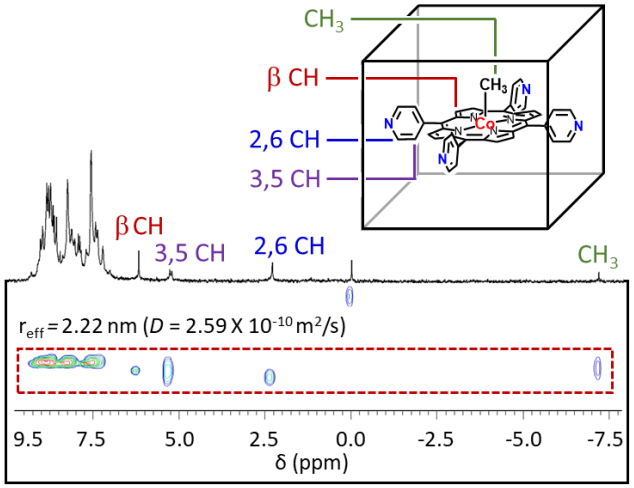

Figure 2. DOSY ^1H NMR spectrum of **(TPyP)Co^{III}Me@1** in CD_3CN at 25 °C. The DOSY-separated 1D spectrum is displayed on top and the corresponding 2D spectrum is shown below with the diffusion coefficient and calculated hydrodynamic radius indicated.

Notably, methylation of the encapsulated Co^{II} complex occurred most effectively in solutions exposed to air and light. Since porphyrin-supported Co^{III}Me complexes are usually degraded under such conditions,[18] the alkylation had first been attempted anaerobically with shielding from light, but only a trace of the Co^{III}Me product was observed by ^1H NMR spectroscopy after 48 h in the presence of 50 equiv of $SnMe_4$ (Figure 4A). Mild heating (40 °C) or exposure to light led to minimal improvements in

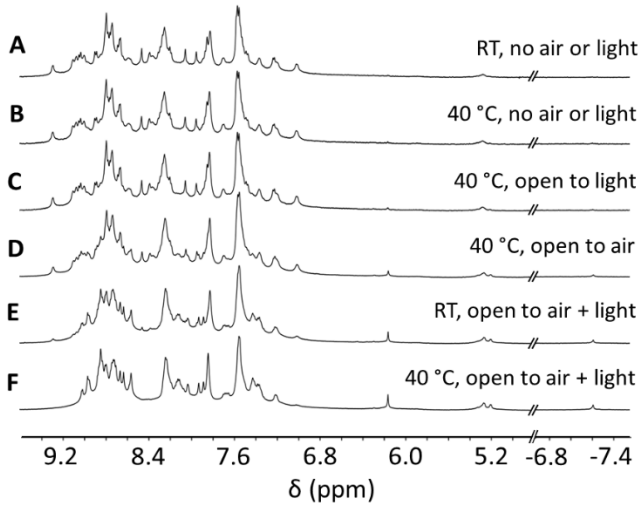

Figure 4. ^1H NMR spectra of CD_3CN solutions of **(TPyP)Co^{II}@1** and SnMe4 (50 equiv) after 48 h under the following reaction conditions: (A) 23 °C free from air and light; (B) 40 °C free from air and light; (C) 40 °C exposed to light and free from air; (D) 40 °C exposed to air and free from light; (E) 23 °C exposed to air and light; (F) 40 °C exposed to air and light.

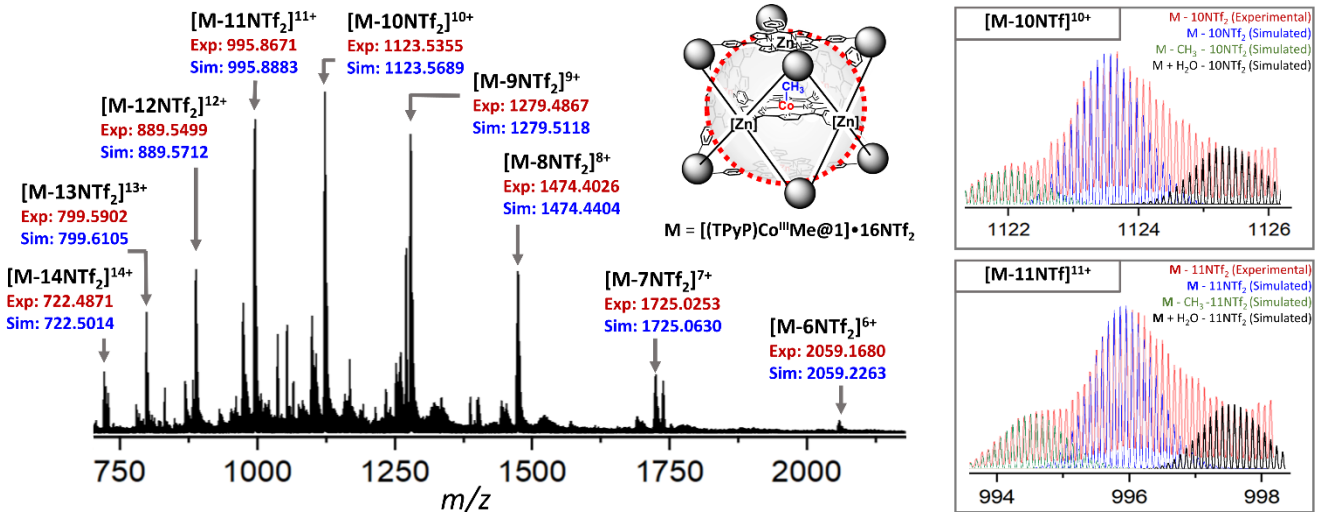

Figure 3. ESI(+)-HRMS characterization of **[(TPyP)Co^{III}Me@1]•16NTf_2**. Signals were observed for the host-guest complex with 2–10 NTf_2^- anions remaining associated. The inset displays peaks observed for **[(TPyP)Co^{III}Me@1•6NTf]$^{10+}$** and **[(TPyP)Co^{III}Me@1•5NTf]$^{11+}$** compared with calculated isotope patterns for this complex with different solvent molecules associated or CH_3 dissociated.

conversion in the absence of air (Figures 4B,C), while exposure of the reaction mixtures to air in the absence of light resulted in considerably greater formation of the $Co^{III}Me$ product (Figure 4D). However, formation of the $Co^{III}Me$ product was most efficient in the presence of both light and air, reaching nearly complete conversion after 48 h when heating to 40 °C was also applied (Figure 4F). These optimized conditions are remarkable since it has long been recognized that porphyrin-supported $Co^{III}Me$ complexes undergo photolytic Co–C homolysis, which in the presence of O_2 leads to irreversible decomposition via formation of unstable $Co^{III}OOMe$ complexes.[18] It is likely that the cage promotes rapid recombination of Co^{II} and $\bullet CH_3$ intermediates after homolysis,[22] inhibiting reaction of the methyl radical with O_2 (*vide infra*).[18a] Similar effects are believed to protect methylcobalamin cofactors from homolytic degradation,[7c] and have also been noted in sterically hindered supramolecular complexes of $Co^{III}Me$ porphyrins with cyclodextrins.[23]

Influence of nanoconfinement on alkylation of Co^{II}. The role of the cubic cage in enabling formation of a $Co^{III}Me$ complex was confirmed in control experiments using monomeric complexes of tetraphenylporphyrin (TPP) and tetrakis(*N*-Me-4-pyridinium)porphyrin (TPyMeP). An attempt at methylation of $(TPP)Co^{II}$ with $SnMe_4$ at 40 °C in $CDCl_3$ (Scheme 2A) was entirely unsuccessful in the presence of air and light (see Figure S16 for monitoring). For comparison, reaction of $(TPP)Co^{III}Cl$ with $SnMe_4$ at 25 °C in $CDCl_3$ in the presence of air and light led to the appearance of a ^1H NMR signal at –4.54 ppm (Figure S15), as reported by Kitano,[21] with a maximum conversion to $(TPP)Co^{III}Me$ of ~77 % reached after 2 h, followed by nearly complete decomposition to the Co^{II} state of the complex after 19 h (Scheme 2B). Thus, $(TPP)Co^{III}Me$ is unstable under these conditions but persists long enough that it should have been observable if the reaction of $(TPP)Co^{II}$ and $SnMe_4$ was effective at forming a Co–C bond. Since chloroform is an effective trap for alkyl radicals, it is conceivable that the failure to form $(TPP)Co^{III}Me$ from

Scheme 2. Conditions for synthesis and decomposition of simple $Co^{III}Me$ porphyrin complexes.

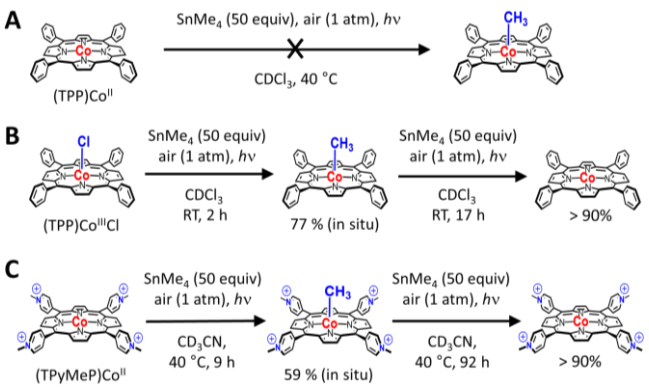

$(TPP)Co^{II}$ is because the $CDCl_3$ solvent intercepts a free $\bullet CH_3$ intermediate prior to its capture by Co^{II}.

Experiments with $[(TPyMeP)Co^{II}]^{4+}$ in CD_3CN provided more direct comparisons with the reactivity of **$(TPyP)Co^{II}$@1**. Alkylation conditions similar to those used for the host-guest complex were effective at partial conversion of $[(TPyMeP)Co^{II}]^{4+}$ into $[(TPyMeP)Co^{III}Me]^{4+}$ (Scheme 2C). However, only ~59 % formation of the methyl complex was reached after 9 h before complete decomposition back to the initial Co^{II} state over 100 h (Figures 5 and S17). When heat was also employed (40 °C), the concentration of methylated Co centers peaked around 1.5 h and degraded within 23 h (Figure S18). Since $[(TPyMeP)Co^{III}Me]^{4+}$ was not formed cleanly using $SnMe_4$, the identity of this $Co^{III}Me$ complex was confirmed by independent synthesis using Me_3O^+ to alkylate the reduced complex $[(TPyMeP)Co^{I}]^{3+}$ (see Supporting Information).[24]

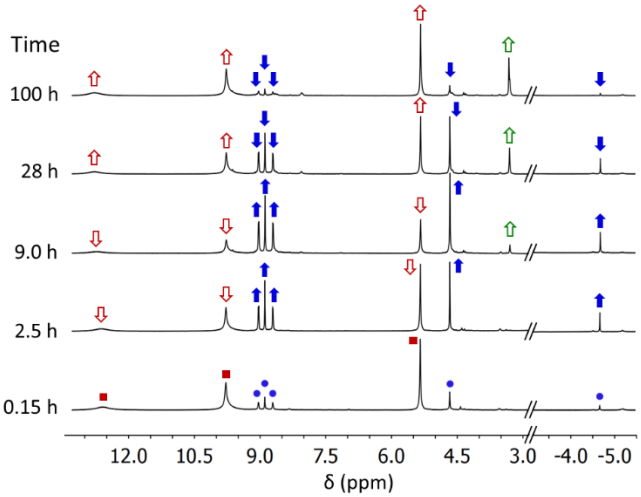

Figure 5. ^1H NMR monitoring of the reaction of $(TPyMeP)Co^{II}$ with excess $SnMe_4$ (50 equiv) in CD_3CN in the presence of air and ambient light at 23 °C. In the earliest spectrum (0.15 h), red squares mark signals of $(TPyMeP)Co^{II}$ and blue dots mark signals of the $(TPyMeP)Co^{III}CH_3$ product. In subsequent spectra, solid blue arrows indicate the growth and disappearance of signals of the $Co^{III}CH_3$ complex, and hollow red arrows mark opposite changes to the signals of the Co^{II} state. Green arrows mark a resonance that grows in at 3.28 ppm that is attributed to formation of MeOH as a product of the decomposition of $(TPyMeP)Co^{III}CH_3$.

The above results reveal that activation of $SnMe_4$ by light and O_2 to form $Co^{III}Me$ products does not require confinement of the initial Co^{II} complex, but that the cube does appear to be necessary to stabilize the product enough to enable full conversion under these conditions. However, the mechanism of alkylation remains an open question. The involvement of light, O_2, and porphyrins suggests that singlet O_2 might be generated as an intermediate that activates $SnMe_4$. Insertion of O_2 into a weak Sn–C bond could form $MeOOSnMe_3$ which could oxidize Co^{II} to a $Co^{III}OR$ complex that might undergo metathesis with additional

$SnMe_4$. However, the partial formation of $Co^{III}Me$ inside the cube even on samples shielded from light (Figure 4D) suggests that an alternative, non-photolytic pathway must also be available. Likewise, the failure to form any (TPP)$Co^{III}Me$ from (TPP)Co^{II} and $SnMe_4$ in $CDCl_3$ suggests that free $\bullet CH_3$ may be involved as part of the alkylation mechanism. Some organotin compounds readily form radicals,[25] but $SnMe_4$ was found to be stable in the absence of cobalt porphyrins, showing no decomposition by ^1H NMR spectroscopy when monitored for 8 days in CD_3CN in the presence of O_2 and light (Figures S22, S23), indicating that the cobalt complex is necessary for activating the organotin reagent. Cobalt(II) porphyrins are known to reversibly bind O_2 to form Co^{III} superoxo complexes that can activate weak covalent bonds,[26] and such reactivity might be enhanced by light.[27] Thus, it is highly plausible that a $Co^{III}–O_2\bullet$ intermediate is involved in activating $SnMe_4$, representing a new example of radical reactivity in a nanoconfined environment. However, aside from the signals of the cobalt complexes and cube, only broad new ^1H NMR resonances appeared when monitoring the methylation reactions in the cube (Figure S3), preventing identification of any tin byproducts. Thus, it is difficult to conjecture with any confidence about the subsequent steps that lead to $Co^{III}Me$ formation, and we caution that our mechanistic interpretations are speculative, especially since more than one pathway may be operative.

The influence of encapsulation on the reactivity of the (TPyP)Co^{II} guest was further probed by comparing the efficiency of alkylation using tetralkyltins of varying sizes ($SnMe_4$, $SnEt_4$, $SnBu_4$). The irregularly shaped apertures of the M_8L_6 cube can be approximated as 10.5 x 5.5 Å ovals (measured between the van der Waals surfaces of the walls) and have been shown to exclude large catalytic substrates from entering the cage,[12b-d,15b] suggesting that bulkier SnR_4 reagents may be ineffective at alkylating the confined Co^{II} site. Thus, the formation of a $Co^{III}Et$ complex was targeted using $SnEt_4$ (Scheme 3), leading to formation of the encapsulated ethyl complex with similar conversion (~ 80 %) as attained for methylation using $SnMe_4$ (≥ 90 %). New signals were observed at –6.19 ppm (multiplet) and –7.68 ppm (triplet, J = 7.7 Hz; Figure S5) for the CH_2 and CH_3 positions of the ethyl ligand inside the cage, and resonances of the TPyP ligand also appeared between 5 and 6.5 ppm, as expected for a bound diamagnetic (TPyP)$Co^{III}Et$ complex.

Scheme 3. Comparison of alkylation of (TPyP)Co^{II}@1 using tetraalkyltin reagents of varying sizes.

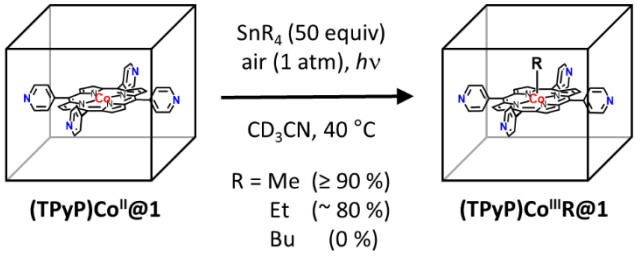

The identity of **(TPyP)Co^{III}Et@1** was also confirmed by ESI-HRMS (Figure S32), though note that the host-guest complex was not fully isolated since the low volatility of $SnEt_4$ (181˚C) prevents easy removal by evaporation. In contrast to the smaller tetraalkyltins, $SnBu_4$ was not effective at alkylating **(TPyP)Co^{II}@1** (Scheme 3) even after several days of heating in the presence of air and light (Figure S21). Presumably, $SnBu_4$ is too large to enter the apertures of the cage or it cannot take on necessary conformations for reaction with the cobalt center in the confined environment.

Stability and Reactivity of (TPyP)Co^{III}Me@Cube. Experiments were performed to further probe the influence of the cubic cage on the reactivity of the encapsulated $Co^{III}Me$ complex. Samples of isolated **(TPyP)Co^{III}Me@1** show no decomposition after seven days in the solid state when stored under N_2 at 25 °C in the absence of light (Figure S3), but decomposition occurs readily upon exposure to air and ambient light. When first attempting to isolate samples of **(TPyP)Co^{III}Me@1**, the host-guest complex was precipitated from the CD_3CN reaction solution using Et_2O and collected by vacuum filtration under air. After 1 h under air, the ^1H NMR spectrum of the resulting product revealed nearly complete decomposition of the $Co^{III}Me$ complex, as evident from the disappearance of its CH_3 resonance. Though decomposition of the methyl complex has proven consistent under these conditions, it has not been possible to confidently identify the resulting cobalt products, in part because varying NMR features have been seen for the decomposition products of different samples.

The sensitivity of the encapsulated $Co^{III}Me$ complex to air in the solid state is surprising given the aerobic conditions needed to efficiently form the methyl complex and the persistence of **(TPyP)Co^{III}Me@1** for several days under these reaction conditions (Figure S19). However, since experiments to form **(TPyP)Co^{III}Me@1** employed a large excess of $SnMe_4$, it was not clear if the $Co^{III}Me$ complex was entirely stable under the reaction conditions or was simply being formed more quickly than it degrades. Thus, the stability of isolated **(TPyP)Co^{III}Me@1** in CD_3CN solution was probed under air vs. N_2 with and without exposure to light. When shielded from light, **(TPyP)Co^{III}Me@1** is quite stable, showing negligible degradation to **(TPyP)Co^{II}@1** over 24 days (Figure S26) even in the presence of oxygen (Figure S27). **(TPyP)Co^{III}Me@1** is much less stable when exposed to light, as expected for a photosensitive complex. The $Co^{III}Me$ complex degrades completely to the Co^{II} state after 10 days of exposure to ambient laboratory lighting under an N_2 atmosphere (Figure S28), and air accelerates the photodecomposition, resulting in complete conversion to the Co^{II} state after 48 h (Figure S29). The 5-fold faster decomposition under air is consistent with known reactivity of (porphyrin)$Co^{III}R$ complexes, for which O_2 can act as an alkyl radical scavenger after photolytic Co–C cleavage, thereby preventing cobalt-alkyl recombination.

However, the relatively long lifetime of **(TPyP)Co^{III}Me@1** even under air and light suggests that encapsulation of the methyl complex may promote faster radical recombination, limiting the ability of O_2 to intercept the released methyl radical.

To further examine how encapsulation influences Co^{III}Me reactivity, samples of **(TPyP)Co^{III}Me@1** were treated with TEMPO (1.5 equiv) in CD_3CN. Even in the absence of air or light, TEMPO reacts with the encapsulated Co^{III}Me complex to form TEMPO-Me (Scheme 4), which was easily identified by ^{1}H NMR spectroscopy (Figure S24).[28] Concomitant conversion of **(TPyP)Co^{III}Me@1** to **(TPyP)Co^{II}@1** was also evident, reaching full conversion to the Co^{II} state after 30 h. Thus, reaction of the encapsulated methyl complex with TEMPO occurs more readily even in the absence of light than reaction with O_2 in the presence of light. This observation suggests that TEMPO can enter the cage to directly abstract the methyl group from cobalt without a separate Co–C homolysis step occurring first.

Scheme 4. Steric influences on the reaction of TEMPO derivatives with (TPyP)Co^{III}Me@1.

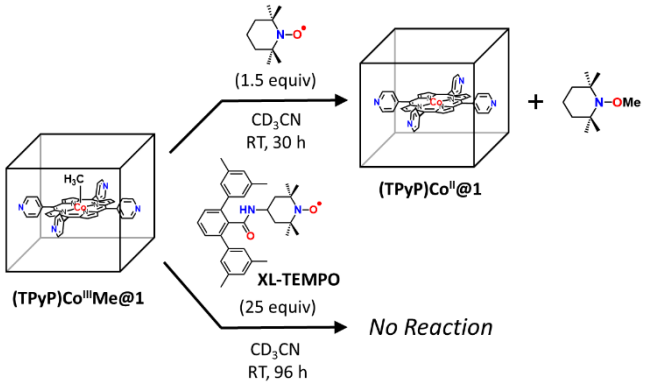

To test whether TEMPO must directly access the Co^{III}Me site to abstract the methyl group, a bulky derivative of TEMPO (XL-TEMPO, Scheme 4) featuring a *m*-terphenyl substituent was prepared and screened for its reactivity with **(TPyP)Co^{III}Me@1**. The bulky TEMPO was prepared by amide condensation between 4-amino-TEMPO and 1,3-bis(3,5-dimethylphenyl)benzoic acid (see Supporting Information), and characterization of XL-TEMPO by NMR, FTIR, and EPR spectroscopy as well as ESI-HRMS (Figures S6, S7, S33, S35, and S37) confirmed the expected identity of this TEMPO derivative. Molecular mechanics calculations provided a structure with dimensions (15.7 x 13.5 x 8.4 Å, Figure S36) that are too large to pass through the apertures of the cube, thus providing a way to test the role of sterics on the reactivity of **(TPyP)Co^{III}Me@1**. The ^{1}H NMR spectrum of **(TPyP)Co^{III}Me@1** remains unchanged after 96 h in CD_3CN solution containing 25 equiv of XL-TEMPO, and no new signals corresponding to XL-TEMPO-Me were observed (Figure S25). These observations confirm that the cube can provide steric control over the reactivity of the bound Co^{III}Me complex, consistent with catalytic studies reported by Reek and de Bruin showing size-selective access of substrates to cobalt or manganese active sites confined in the cube.[12b-d,15b]

Summary and Conclusions

In summary, encapsulation of (TPyP)Co^{II} in a large self-assembled nanocage enabled the discovery of a new method for forming cobalt-alkyl complexes directly from the Co^{II} state of the porphyrin complex, thus complementing previous alkylation methods that require initial oxidation or reduction of cobalt to its Co^{III} or Co^{I} states prior to respective treatment with nucleophilic or electrophilic alkyl-transfer reagents. Interestingly, the newly discovered alkylation methodology uses light and O_2 to promote the reaction between SnR_4 and cobalt, which is surprising since these conditions usually cause decomposition of Co^{III}–alkyl complexes supported by porphyrin ligands. Indeed, the stabilizing effects of encapsulation appear to be essential for formation of the alkyl complexes. Free porphyrin complexes did not undergo complete cobalt-alkyl formation under analogous conditions, though partial conversion could be obtained in a sufficiently unreactive solvent.

The role of encapsulation in controlling the reactivity of the (TPyP)Co guest was confirmed by experiments examining the efficiency of alkylation using different SnR_4 reagents or the stability of the resulting Co^{III}Me complex under various conditions. Together, these experiments indicate that the cube can prevent access of bulky reagents (e.g., $SnBu_4$, XL-TEMPO) to the cobalt center and that encapsulation also stabilizes the cobalt-alkyl complex by promoting radical recombination under conditions that stimulate Co–C homolysis. This latter feature is key to the clean formation of the confined alkyl complexes in the presence of air and light, suggesting that porous structures show considerable promise for controlling the reactivity between transition metals and free radicals to enable new chemistry that is not possible in free solution.

ASSOCIATED CONTENT

Supporting Information. Synthetic and experimental procedures; ^{1}H NMR, ^{13}C{^{1}H} NMR, DOSY NMR, EPR, and ESI(+)-MS characterization data. These materials are available free of charge via the Internet.

AUTHOR INFORMATION

Corresponding Author

* ml1353@chem.rutgers.edu

Author Contributions

All authors have given approval to the final version of the manuscript.

Notes

The authors declare no competing financial interests.

ACKNOWLEDGMENT

The authors acknowledge Rutgers, The State University of New Jersey and the ACS Petroleum Research Fund (PRF grant #61015-DNI3) for financial support of this research. DAR acknowledges BASF for fellowship support. The authors also thank Souvik Mandel from Rutgers, The State University of New Jersey and Dr. Donald Hirsch from The College of New Jersey for assistance in acquiring EPR spectra.

REFERENCES

1. (a) Griller, D.; Ingold, K. U. Persistent carbon-centered radicals. *Acc. Chem. Res.* **1976**, *9*, 13-19. DOI: 10.1021/ar50097a003; (b) Studer, A.; Curran, D. P. Catalysis of Radical Reactions: A Radical Chemistry Perspective. *Angew. Chem. Int. Ed.* **2016**, *55*, 58–102. DOI: 10.1002/anie.201505090; (c) Kerr, J. A. Bond Dissociation Energies by Kinetic Methods. *Chem. Rev.* **1966**, *66*, 465–500. DOI: 10.1021/cr60243a001; (d) Rozantsev, E. G.; Loshadkin, D. V. The History and Modern Problems of Free Radical Chemistry. 100 Years of Free Radical Chemistry. *Des. Monomers Polym.* **2001**, *4*, 281–300. DOI: 10.1163/156855501753210781.

2. (a) Bour, J. R; Ferguson, D. M.; McClain, E. J.; Kampf, J. W.; Sanford, M. S. Connecting Organometallic Ni(III) and Ni(IV): Reactions of Carbon-Centered Radicals with High-Valent Organonickel Complexes. *J. Am. Chem. Soc.* **2019**, *141*, 8914-8920. DOI: 10.1021/jacs.9b02411; (b) Gonzalez, M. I.; Gygi, D.; Qin, Y.; Zhu, Q.; Johnson, E. J.; Chen, Y.-S.; Nocera, D. G. Taming the Chloride Radical: Enforcing Steric Control over Chloride-Radical-Mediated C-H Actviation. *J. Am. Chem. Soc.* **2022**, *144*, 1464-1472. DOI: 10.1021/jacs.1c13333; (c) Demarteau, J.; Debuigne, A.; Detrembleur, C. Organocobalt Complexes as Sources of Carbon-Centered Radicals for Organic and Polymer Chemistries. *Chem. Rev.* **2019**, *119*, 6906–6955. DOI: 10.1021/acs.chemrev.8b00715; (d) Epping, R. F. J; Vesseur, D.; Zhou, M.; de Bruin, B. Carbene Radicals in Transition-Metal-Catalyzed Reactions. *ACS Catal.* **2023**, *13*, 5428–5448. DOI: 10.1021/acscatal.3c00591; (e) Lyaskovskyy, V.; Suarez, A. I. O.; Lu, H.; Jiang, H.; Zhang, X. P.; de Bruin, B.; Mechanism of Cobalt (II) Porphyrin-Catalyzed C-H Amination with Organic Azides: Radical Nature and H-Atom Abstraction Ability of the Key Cobalt(III)-Nitrene Intermediates. *J. Am. Chem. Soc.* **2011**, *133,* 12264-12273. DOI: 10.1021/ja204800a; (f) Shields, B. J.; Doyle, A. G. Direct C(sp^3)–H Cross Coupling Enabled by Catalytic Generation of Chlorine Radicals. *J. Am. Chem Soc.* **2016**, *138*, 12719–12722. DOI: 10.1021/jacs.6b08397.

3. (a) Ananikov, V. P. Nickel: The "Spirited Horse" of Transition Metal Catalysis. *ACS. Catal.* **2015**, *5*, 1964-1971. DOI: 10.1021/acscatal.5b00072; (b) Koppenol, W. H. The centennial of the Fenton reaction. *Free Radic. Biol. Med.* **1993**, *15*, 645-651. DOI: 10.1016/0891-5849(93)90168-T; (c) Gu, Q.-S.; Li, Z.-L. ; Liu, X.-Y. Copper(I)-Catalyzed Asymmetric Reactions Involving Radicals. *Acc. Chem. Res.* **2020**, *53*, 170-181. DOI: 10.1021/acs.accounts.9b00381; (d) Akhtar, R.; Zahoor, A. F.; Rasool, N.; Ahmad, M.; Ali, K. G. Recent trends in the chemistry of the Sandmeyer reaction: a review. *Mol. Divers.* **2022**, *26*, 1837-1873. DOI: 10.1007/s11030-021-10295-3. (e) Ephritikhine, M. A New Look at the McMurry Reaction. *Chem. Commun.* **1998**, 2549–2554. DOI: 10.1039/a804394i.

4. (a) Gunay, A.; Theopold, K. H. C–H Bond Activations by Metal Oxo Compounds. *Chem. Rev.* **2010**, *110*, 1060–1081. DOI: 10.1021/cr900269x; (b) Liu, W.; Groves, J. T. Manganese Catalyzed C-H Halogenation. *Acc. Chem. Res.* **2015**, *48*, 1727-1735. DOI: 10.1021/acs.accounts.5b00062; (c) Rajeev, A.; Balamurugan, M.; Sankaralingam, M. Rational Design of First-Row Transition Metal Complexes as the Catalysts for Oxidation of Arenes: A Homogeneous Approach. *ACS Catal.* **2022**, *12*, 9953–9982. DOI: 10.1021/acscatal.2c01928; (d) Saint-Denis, T. G.; Zhu, R.-Y.; Chen, G.; Wu, Q.-F.; Yu, J.-Q. Enantioselective C(sp^3)-H bond activation by chiral transition metal catalysts. *Science*. **2018**, *359*, eaao4798. DOI: 10.1126/science.aao4798; (e) Costas, M. Selective C–H Oxidation Catalyzed by Metalloporphyrins. *Coord. Chem. Rev.* **2011**, *255*, 2912–2932. DOI: 10.1016/j.ccr.2011.06.026.

5. (a) Ye, S.; Xiang, T.; Li, X.; Wu, J. Metal-Catalyzed Radical-Type Transformation of Unactivated Alkyl Halides with C–C Bond Formation under Photoinduced Conditions. *Org. Chem. Front.* **2019**, *6*, 2183–2199. DOI: 10.1039/C9QO00272C; (b) Liu, D.; Li, Y.; Qi, X.; Liu, C.; Lan, Y.; Lei, A. Nickel-Catalyzed Selective Oxidative Radical Cross-Coupling: An Effective Strategy for Inert Csp^3–H Functionalization. *Org. Lett.* **2015**, *17*, 998–1001. DOI: 10.1021/acs.orglett.5b00104; (c) Diccianni, J.; Lin, Q.; Diao, T. Mechanisms of Nickel-Catalyzed Coupling Reactions and Applications in Alkene Functionalization. *Acc. Chem. Res.* **2020**, *53*, 906–919. DOI: 10.1021/acs.accounts.0c00032; (d) Iqbal, J.; Bhatia, B.; Nayyar, N. K. Transition Metal- Promoted Free-Radical Reactions in Organic Synthesis: The Formation of Carbon-Carbon Bonds. *Chem. Rev.* **1994**, *94*, 519-564. DOI: 10.1021/cr00026a008.

6. (a) Bar, G.; Parsons, A. F. Stereoselective radical reactions. *Chem. Soc. Rev.* **2003**, *32,* 251-263. DOI: 10.1039/B111414J; (b) Walling, C. Some Properties of Radical Reactions Important in Synthesis. *Tetrahedron*, **1985**, *41*, 3887-3900. DOI: 10.1016/S0040-4020(01)97172-8; (c) Ruffoni, A.; Mykura, R.C.; Bietti, M.; Leonori, D. The interplay of polar effects in controlling the selectivity of radical reactions. *Nat. Synth.* **2022,** *1,* 682-695. DOI: 10.1038/s44160-022-00108-2 (d) Hofmann, J.; Clark, T.; Heinrich, M. R. Strongly Directing Substituents in the Radical Arylation of Substituted Benzenes. *J. Org. Chem.* **2016**, *81,* 9785-9791. DOI: 10.1021/acs.joc.6b01840.

7. (a) Newcomb, M.; Zhang, R.; Chandrasena, R. E. P.; Halgrimson, J. A.; Horner, J. R.; Makris, T. M.; Sligar, S. G. Cytochrome P450 Compound I. *J. Am. Chem. Soc.* **2006**, *128*, 4580–4581. DOI: 10.1021/ja060048y; (b) Mamun, A. A.; Toda, M. J.; Lodowski, P.; Kozlowski, P. M. Photolytic Cleavage of Co–C Bond in Coenzyme B_{12}-Dependent Glutamate Mutase. *J. Chem. Phys. B.* **2019**, *123*, 2585–2598. DOI: 10.1021/acs.jpcb.8b07547; (c) Jarrett, J. T.; Drennan, C. L.; Amaratunga, M.; Scholten, J. D.; Ludwig, M. L.; Matthews, R. G. A Protein Radical Cage Slows Photolysis of Methylcobalamin in Methionine Synthase from *Escherichia Coli*. *Bioorg. Med. Chem.* **1996**, *4*, 1237–1246. DOI: 10.1016/0968-0896(96)00119-8; (d) Rittle, J.; Green, M. T. Cytochrome P450 Compound I: Capture, Characterization, and C-H Bond Activation Kinetics. *Science* **2010**, *330*, 933–937. DOI: 10.1126/science.1193478. (e) Zhou, Q.; Chin, M.; Fu, Y.; Liu, P.; Yang, Y. Stereodivergent atom-transfer radical cyclization by engineered cytochromes P450. *Science.* **2021,** *374,* 1612-1616. DOI: 10.1126/science.abk1603; (f) Jensen, K. P.; Ryde, U. How the Co-C Bond is Cleaved in Coenzyme B_{12} Enzymes: A Theoretical Study. *J. Am. Chem. Soc.* **2005**, *127*, 9117-9128. DOI: 10.1021/ja050744i.

8. (a) Huang, X.; Groves, J. T. Beyond ferryl-mediated hydroxylation: 40 years of the rebound mechanism and C-H activation. *J. Biol. Inorg. Chem.* **2017**, *22*, 185-207. DOI: 10.1007/s00775-016-1414-3; (b) Sirajuddin, S.; Rosenzweig, A. C. Enzymatic Oxidation of Methane. *Biochemistry,* **2015**, 54, 2283-2294. DOI: 10.1021/acs.biochem.5b00198; (c) Matthews, M. L.; Krest, C. M.; Barr, E. W.; Vaillancourt, F. H.; Walsh, C. T.; Green, M. T.; Krebs, C.; Bollinger Jr., J. M. Substrate-Triggered Formation and Remarkable Stability of the C–H Bond-Cleaving Chloroferryl Intermediate in the Aliphatic Halogenase, SyrB2. *Biochemistry* **2009**, *48*, 4331 – 4343. DOI: 10.1021/bi900109z.

9. (a) Gruber, K.; Puffer, B.; Kräutler, B. Vitamin B_{12}-Derivatives—Enzyme Cofactors and Ligands of Proteins and Nucleic Acids. *Chem. Soc. Rev.* **2011**, *40*, 4346-4363. DOI: 10.1039/c1cs15118e; (b) Halpern, J. Mechanisms of Coenzyme B_{12}-Dependent Rearrangements. *Science.* **1985**, *227*, 869-875. DOI: 10.1126/science.2857503.

10. (a) Chakrabarty, R.; Mukherjee, P. S.; Stang, P. J. Supramolecular Coordination: Self-Assembly of Finite Two- and Three-Dimensional Ensembles. *Chem. Rev.* **2011**, *111*, 6810–6918. DOI: 10.1021/cr200077m; (b) Montá-González, G.; Sancenón, F.; Martínez-Máñez, R.; Martí-Centelles, V. Purely Covalent Molecular Cages and Containers for Guest Encapsulation. *Chem. Rev.* **2022,** *122,* 13636-13708. DOI: 10.1021/acs.chemrev.2c00198; (c) Yang, X.; Ullah, Z.; Stoddart, J. F.; Yavuz, C. T. Porous Organic Cages. *Chem. Rev.* **2023,** *123*, 4602-4634. DOI: 10.1021/acs.chemrev.2c00667; (d) Saha, R.; Mondal, B.; Mukherjee, P. S. Molecular Cavity for Catalysis and Formation of Metal Nanoparticles for Use Catalysis. *Chem. Rev.* **2022**, *122*, 12244-12307. DOI: 10.1021/acs.chemrev.1c00811; (e) Rizzuto, F. J.; von Krbek, L. K. S.; Nitschke, J. R. Strategies for binding multiple guests in metal-organic cages. *Nat. Rev. Chem.* **2019**, *3,* 204-222. DOI: 10.1038/s41570-019-0085-3; (f) Percástegui, E. G.; Jancik, V. Cordination-driven assemblies based on meso-substitued porphyrins: Metal-organic cages and a new type of meso-metallaporphyrin macrocycles. *Coord. Chem. Rev.* **2020**, *407,* 213165. DOI: 10.1016/j.ccr.2019.213165; (g) Cook, T. R.; Stang, P. J. Recent Developments in the Preparation and Chemistry of Metallacycles and Metallacages via Coordination. *Chem. Rev.* **2015,** 115*, 7001-7045.* DOI: 10.1021/cr5005666.

11. (a) Yaghi, O. M.; O'Keeffe, M.; Ockwig, N. W.; Chae, H. K.; Eddaoudi, M.; Kim, J. Reticular Synthesis and the Design of New Materials. *Nature* **2003**, *423*, 705–714. DOI: 10.1038/nature01650; (b) Zhang, X.; Chen, Z.; Liu, X.; Hanna, S. L.; Wang, X.; Taheri-Ledari, R.; Maleki, A.; Li, P.; Farha, O. K. A historical overview of the activation and porosity of metal-organic frameworks. *Chem. Soc. Rev.* **2020,** *49,* 7406-7427. DOI: 10.1039/D0CS00997K; (c) Ji, Z.; Wang, H.; Canossa, S.; Wuttke, S.; Yaghi, O. M. Pore Chemistry of Metal-Organic Frameworks. *Adv. Funct. Mater.* **2020**, *30*, 2000238. DOI: 10.1002/adfm.202000238; (d) Wu, L.; Fan, W.; Wang, X.; Lin, H.; Tao, J.; Liu, Y.; Deng, J.; Jing, L.; Dai, H. Methane Oxidation over the Zeolites-Based Catalysts. *Catalysts*. **2023**, *13*, 604. DOI: 10.3390/catal13030604.

12. (a) Das, A.; Mandal, I.; Venkatramani, R.; Dasgupta, J. Ultrafast Photoactivation of C─H Bonds inside Water-Soluble Nanocages. *Sci. Adv.* **2019**, *5*, eaav4806. DOI: 10.1126/sciadv.aav4806; (b) Otte, M.; Kuijpers, P. F.; Troeppner, O.; Ivanović-Burmazović, I.; Reek, J. H.; de Bruin, B. Encapsulated Cobalt-Porphyrin as a Catalyst for Size-Selective Radical-Type Cyclopropanation Reactions. *Chem. Eur. J.* **2014**, *20*, 4880–4884. DOI: 10.1002/chem.201400055; (c) Mouarrawis, V.; Bobylev, E. O.; de Bruin, B.; Reek, J. H. A Novel M_8L_6 Cubic Cage That Binds Tetrapyridyl Porphyrins: Cage and Solvent Effects in Cobalt-Porphyrin-Catalyzed Cyclopropanation Reactions. *Chem. Eur. J.* **2021**, *27*, 8390–8397. DOI: 10.1002/chem.202100344; (d) Otte, M.; Kuijpers, P. F.; Troeppner, O.; Ivanović-Burmazović, I.; Reek, J. H.; De Bruin, B. Encapsulation of Metalloporphyrins in a Self-Assembled Cubic M_8L_6Cage: A New Molecular Flask for Cobalt-Porphyrin-Catalysed Radical-Type Reactions. *Chem. Eur. J.* **2013**, *19*, 10170–10178. DOI: 10.1002/chem.201301411.

13. (a) Hasegawa, S.; Meichsner, S. L.; Holstein, J. J.; Ananya B.; Kasanmascheff, M.; Clever, G. H. Long-Lived C_{60} Radical Anion Stabilized inside an Electron-Deficient Coordination Cage. *J. Am. Chem. Soc.* **2021**, *143*, 9718–9723. DOI: 10.1021/jacs.1c02860; (b) Lü, B.; Chen, Y.; Li, P.; Wang, B.; Müllen, K.; Yin, M. Stable Radical Anions Generated from a Porous Perylenediimide Metal-Organic Framework for Boosting Near-Infrared Photothermal Conversion. *Nat. Commun.* **2019**, *10,* 767. DOI: 10.1038/s41467-019-08434-4; (c) Liu, Q.-K.; Ma, J.-P.; Dong, Y.-B. Adsorption and Separation of Reactive Aromatic Isomers and Generation and Stabilization of Their Radicals within Cadmium(II)–Triazole Metal–Organic Confined Space in a Single-Crystal-To-Single-Crystal Fashion. *J. Am. Chem. Soc.* **2010**, *132*, 7005–7017. DOI: 10.1021/ja101807c; (d) Liu, Y.; Shi, J.; Chen, Y.; Ke, C.-F. A Polymeric Pseudorotaxane Constructed from Cucurbituril and Aniline, and Stabilization of Its Radical Cation. *Angew. Chem. Int. Ed.* **2008**, *47*, 7293–7296. DOI: 10.1002/anie.200802805; (e) Eelkema, R.; Maeda, K.; Odell, B.; Ackermann, L. Radical Cation Stabilization in a Cucurbituril Oligoaniline Rotaxane. *J. Am. Chem. Soc.* **2007**, *129*, 12384–12385. DOI: 10.1021/ja074997i; (f) Harada, Y.; Kusaka, S.; Nakajo, T.; Kumagai, J.; Kim, C. R.; Shim, J. Y.; Hori, A.; Ma, Y.; Matsuda, R. Stabilization of Radical Active Species in a MOF Nanospace to Exploit Unique Reaction Pathways. *Chem. Comm.* **2021**, *57*, 12115–12118. DOI: 10.1039/D1CC04267J.

14. (a) Galan, A.; Ballester, P. Stabilization of Reactive Species by Supramolecular Encapsulation. *Chem. Soc. Rev.* **2016**, *45*, 1720–1737. DOI: 10.1039/c5cs00861a; (b) Kawamichi, T.; Haneda, T.; Kawano, M.; Fujita, M. X-Ray Observation of a Transient Hemiaminal Trapped in a Porous Network. *Nature* **2009**, *461*, 633–635. DOI: 10.1038/nature08326; (c) Schwarzmaier, C.; Schindler, A.; Heindl, C.; Scheuermayer, S.; Peresypkina, E. V.; Virovets, A. V.; Neumeier, M.; Gschwind, R.; Scheer, M. Stabilization of Tetrahedral P_4 and As_4 Molecules as Guests in Polymeric and Spherical Environments. *Angew. Chem. Int. Ed.* **2013**, *52*, 10896–10899. DOI: 10.1002/anie.201306146; (d) Mal, P.; Breiner, B.; Rissanen, K.; Nitschke, J. R. White Phosphorus Is Air-Stable within a Self-Assembled Tetrahedral Capsule. *Science* **2009**, *324*, 1697–1699. DOI: 10.1126/science.1175313.

15. (a) Lee, S. J.; Cho, S.-H.; Mulfort, K. L.; Tiede, D. M.; Hupp, J. T.; Nguyen, S. T. Cavity-Tailored, Self-Sorting Supramolecular Catalytic Boxes for Selective Oxidation. *J. Am. Chem. Soc.* **2008**, *130*, 16828–16829. DOI: 10.1021/ja804014y; (b) Kuijpers, P. F.; Otte, M.; Dürr, M.; Ivanović-Burmazović, I.; Reek, J. N. H.; de Bruin, B. A Self-Assembled Molecular Cage for Substrate-Selective Epoxidation Reactions in Aqueous Media. *ACS Catal.* **2016**, *6*, 3106–3112. DOI: 10.1021/acscatal.6b00283; (c) Chen, S.; Chen, L.-J. Metal-Organic Cages: Applications in Organic Reactions. *Chemistry* **2022**, 4, 494-519. DOI: 10.3390/chemistry4020036; (d) Hong, C. M., Bergman, R. G.; Raymond, K. N.; Toste, F. D. Self-Assembled Tetrahedral Hosts as Supramolecular Catalysts. *Acc. Chem. Res.* **2018**, *51*, 2477-2455. DOI: 10.1021/acs.accounts.8b00328.

16. (a) Lu, H.; Dzik, W. I.; Xu, X.; Wojtas, L.; de Bruin, B.; Zhang, X. P. Experimental Evidence for Cobalt(III)-Carbene Radicals: Key Intermediates in Cobalt(II)-Based Metalloradical Cyclopropanation. *J. Am. Chem. Soc.* **2011**, *133*, 8518–8521. DOI: 10.1021/ja203434c; (b) Snabilié, D. D.; Meeus, E. J.; Epping, R. F. J.; He, Z.; Zhou, M.; De Bruin, B. Understanding Off-Cycle and Deactivation Pathways in Radical-Type Carbene Transfer Catalysis. *Chem. Eur. J.* **2023**, *29,* e202300336. DOI: 10.1002/chem.202300336.

17. Lv, X-L.; Wang, K.; Wang, B.; Su, J.; Zou, X.; Xie, Y.; Li, J.-R.; Zhou, H.-C. A Base-Resistant Metalloporphyrin Metal–Organic Framework for C–H Bond Halogenation. *J. Am. Chem. Soc.* **2017**, *139*, 211–217. DOI: 10.1021/jacs.6b09463.

18. (a) Kendrick, M. J.; Al-Akhdar, W. Preparation and Characterization of (Alkylperoxo)Cobalt(III) Porphyrins: First Direct Evidence for Metal-Carbon Bond Homolysis in Dioxygen Insertion Reactions. *Inorg. Chem.* **1987**, *26*, 3971–3972. DOI: 10.1021/ic00271a001. (b) Mikolaiski, W.; Baum, G.; Massa, W.; Hoffmann, R. W. Bildung Und Struktur von Allylperoxy-Cobalt(III)-Tetraphenyl-Porphyrin. *J. Organomet. Chem.* **1989**, *376*, 397–405. DOI: 10.1016/0022-328X(89)85149-6. (c) Mandal, D.; Bhuyan, M.; Laskar, M.; Gupta, B. D. Co–C Bond Homolysis: Reactivity Difference between Alkyl- and Benzylcobaloximes. *Organometallics,* **2007**, *26*, 2795–2798. DOI: 10.1021/om070053q; (d) Lodowski, P.; Jaworska, M.; Garabato, B. D.; Kozlowski, P. M. Mechanism of Co–C Bond Photolysis in Methylcobalamin: Influence of Axial Base. *J. Phys. Chem. A*. **2015**, *119*, 3913–3928. DOI: 10.1021/jp5120674.

19. Schrauzer, G. N.; Deutsch, E. Reactions of Cobalt(I) Supernucleophiles. The Alkylation of Vitamin B12s, Cobaloximes(I), and Related Compounds. *J. Am. Chem. Soc.* **1969**, *91*, 3341–3350. DOI: 10.1021/ja01040a041. (b) Hisanobu, O.; Watanabe, E.-i.; Norihisa K.; Yoshida, Z.-i. Synthesis and Properties of Organocobalt(III)Octaethylporphyrins. *Bull. Chem. Soc. Jpn.* **1976**, *49*, 2529–2536. DOI: 10.1246/bcsj.49.2529.

20. Clarke, D. A.; Dolphin, D.; Grigg, R.; Johnson, A. W.; Pinnock, H. A. Alkyl-, aryl-, and acyl-metal(III) complexes of aetioporphyrin I. *J. Chem. Soc. C.* **1968**, 881-885. DOI: 10.1039/J39680000881; (b) Callot, H. J.; Metz, F. Acid-catalyzed intramolecular cobalt to nitrogen aryl migration and intramolecular reverse reaction in cobalt porphyrins. Synthesis of N-phenyl porphyrins. *J. Chem. Soc., Chem. Commun.* **1982**, 947-948. DOI: 10.1039/C39820000947.

21. Fukuzumi, S.; Kitano, T. Reductive Alkylation of Cobalt(III) Porphyrin by Tetraalkyltin Compounds and Alkylcobalt(III) Complexes. *Inorg. Chem.* **1990**, *29*, 2558–2559. DOI: 10.1021/ic00339a005.

22. Barry, J. T.; Berg, D. J.; Tyler, D. R. Radical Cage Effects: The Prediction of Radical Cage Pair Recombination Efficiencies Using Microviscosity across a Range of Solvent Types. *J. Am Chem. Soc.* **2017**, *139*, 14399–14405. DOI: 10.1021/jacs.7b04499.

23. Imabeppu, K.; Kuwano, H.; Yutani, E.; Kitagishi, H.; Kano, K. Photoinduced Homolysis of Alkyl–Cobalt(III) Bonds in a Cyclodextrin Cage. *Eur. J. Inorg. Chem.* **2016**, *2016*, 1784–1789. DOI: 10.1002/ejic.201600208.

24. Blackburn, P. T.; Mansoor, I. F.; Dutton, K. G.; Tyryshkin, A. M.; Lipke, M. C. Accessing three oxidation states of cobalt in M_6L_3 nanoprisms with cobalt-porphyrin walls. *Chem. Comm.* **2021**, *57, 11342-11345.* DOI: 10.1039/D1CC04860K.

25. Crespi, S.; Fagnoni, M. Generation of Alkyl Radicals: From the Tyranny of Tin to the Photon Democracy. *Chem. Rev.* **2020**, *120*, 9790–9833. DOI: 10.1021/acs.chemrev.0c00278.

26. (a) Collman, J. P.; Brauman, J. I.; Doxsee, K. M.; Halbert, T. R.; Hayes, S. E.; Suslick, K. S. Oxygen Binding to Cobalt Porphyrins. *J. Am. Chem. Soc.* **1978**, *100*, 2761–2766. DOI: 10.1021/ja00477a031; (b) Collman, J. P.; Brauman, J. I.; Halbert, T. R.; Suslick, K. S. Nature of O_2 and CO Binding to Metalloporphyrins and Heme Proteins. *Proc. Natl. Acad. Sci. U.S.A.* **1976**, *73*, 3333–3337. DOI: 10.1073/pnas.73.10.3333. (c) Sacramento, J. J. D.; Goldberg, D. P. The hydrogen atom transfer reactivity of a porphyrinoid cobalt superoxide complex. *Chem. Commun*. **2019**, *55*, 913 – 916. DOI: 10.1039/C8CC08453J (d) Wang, C.-C.; Chang, H.-C.; Lai, Y.-C.; Fang, H.; Li, C.-C.; Hsu, H.-K.; Li, Z.-Y.; Lin, T.-S.; Kuo, T.-S.; Neese, F.; Ye, S.; Chiang, Y.-W.; Tsai, M.-L.; Liaw, W.-F.; Lee, W.-Z. A Structurally Characterized Nonheme Cobalt–Hydroperoxo Complex Derived from Its Superoxo Intermediate via Hydrogen Atom Abstraction. *J. Am. Chem. Soc.* **2016**, *138*, 14186–14189. DOI: 10.1021/jacs.6b08642.

27. (a) Jung, J.; Ohkubo, K.; Prokop-Prigge, K. A.; Neu, H. M.; Goldberg, D. P.; Fukuzumi, S. Photochemical Oxidation of a Manganese(III) Complex with Oxygen and Toluene Derivatives to Form a Manganese(V)-Oxo Complex *Inorg. Chem.* **2013**, *52*, 13594 – 13604. DOI: 10.1021/ic402121j. (b) Jung, J.; Neu, H. M.; Leeladee, P.; Siegler, M. A.; Ohkubo, K.; Goldberg, D. P.; Fukuzumi, S. Photocatalytic Oxygenation of Substrates by Dioxygen with Protonated Manganese(III) Corrolazine. *Inorg. Chem.* **2016**, *55*, 3218 – 3228. DOI: 10.1021/acs.inorgchem.5b02019

28. Schultz, J. W.; Fuchigami, K.; Zheng, B.; Rath, N. P.; Mirica, L. M. Isolated Organometallic Nickel(III) and Nickel(IV) Complexes Relevant to Carbon–Carbon Bond Formation Reactions. *J. Am. Chem. Soc.* **2016**, *138*, 12928–12934. DOI: 10.1021/jacs.6b06862.

TOC Graphic

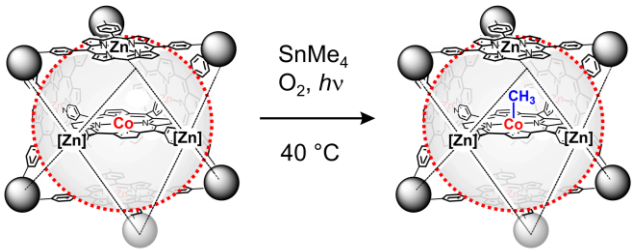

Encapsulated (TPyP)Co^{II} leads to Stabilized (TPyP)$Co^{III}Me$